The Effect of Partial Substitution of Ge-S-Cd Alloys on the Density of Energy States

[1]Zainab Abd Al-hadi* **[2]Kareem A. Jasim**

[1,2]Department of Physics, College of Education for Sciences Ibn-AL-Haitham, University of Baghdad, Baghdad, Iraq.

*Corresponding Author. zainab.abd2104m@ihcoedu.uobaghdad.edu.iq

Abstract

Five samples of the ternary alloy Ge-S-Cd were created using the melting point method, and the effects of partially substituting cadmium for germanium were determined. and partial substitution of germanium by cadmium was used to study the change in electrical conductivity. Electrical experiments were performed on $Ge_{35-x}S_{65}Cd_x$ ternary alloy with x = 0, 5, 10, 15, and 20. It was discovered that the conductivity (σ_{dc}) rises with rising temperature in all samples under experiment. This confirms that the samples have semiconductor behavior. It has been observed that there are three regions of electrical conductivity in the electrical conductivity curve at low, moderate, and high temperatures. The preexponential elements and effective energies of each of the three conduction regions were calculated for each of the Cadmium values. It was found that all of them were impacted by a rise in the value of cadmium in the ingot. A numerical analysis of the conductivity equation was also performed to calculate the energy of the expanding states' density in local states and at the Fermi level. It has been observed that all of the values of samples change with the rising value of cadmium concentration.

Keywords: Melting point method, Electrical conductivity, ternary, numerical analysis, energy density of the extended states, ternary alloy.

1. Introduction

Often referred to as non-oxide chemicals, chalcogenides including at most one chalcogenide component, like Se, S, and Te, relating to set 16 of O [1], mixed with electro-positive components, mainly components from set 15 Sb, Bi As. And set 14 Si, Sn, Pb, Ge, and chalcogenides exhibit a special set of features that have led to their widespread use for nonvolatile device uses like optical data storage, CD-RW and DVD-RAM, conductive random access memory, or phase change of RAM [2]. Recently, due to the lack of continuity, the massive-electronic and the lack of continuity in particular the Ovonic Threshold Switching (OTS) mechanism, some chalcogenides glass below use of electric fields, the last is among the materials with the best potential for use as a novel determinant element in 3D memory matrix [3, 4]. In addition, with their high significant optical nonlinearity and an infrared window [5, 6], The creation of novel

infrared (MIR) components such as superconducting laser sources, optical sensors, infrared microlens arrays, and optical integrated circuits is another possibility made possible by chalcogenide glasses [7, 8]. It has already been shown that amorphous semiconductors have the potential to be used in optical applications. The inherent complexity of highly disordered materials prevents structural characterization and theoretical modeling, which is why glass science advancements lag behind those in crystallography [9]. As of now, Ge-As-Se waveguides [12], As_2S_3 and As_2Se_3 fibers [10], and As_2Se_3 are the main chalcogenides that have been used to generate state-of-the-art MIR(SCs).

Electrical conductivity in chalcogenide glasses is thermally activated and increases exponentially as the absolute temperature decreases. [13, 14] According to Abkowitz, conductance is unaffected by insufficiently low frequencies, and conductance typically rises sharply with frequency. At higher frequencies, the conductivity of glass can be calculated as the sum of a frequency-dependent component with a range as well as a frequency-independent component. This distinction was already covered. [13] Attributed the frequency-dependent portion to hopping and the frequency-independent portion to intrinsic bandwidth delivery. At frequencies up to 10 kHz in either DC or AC, the latter contribution predominates. Becker and Webb [14] looked at the DC conductivity of several chalcogenide beakers and found that the patterns of conductivity are linear at lower temperatures. This means that the materials are semiconducting. Five ternary Ge-S-Cd alloy samples will be created by the melting point, along with its impacts on the electrical conductivity and energy density mechanisms of the stretched states, in situ states, and at the Fermi level. We also examine changes in continuous electrical conductivity upon partial replacement of germanium with cadmium.

2. Materials and Methods

The bulk $Ge_{35-x}S_{65}Cd_x$ ternary alloy with x = 0, 5, 10, 15, and 20 was made by the molten point technique using the mechanical milling method. Higher-quality powders of Ge, S, and Cd at 99.999% were employed to create the ternary $Ge_{35-x}S_{65}Cd_x$ alloy. The input materials were weighed in stoichiometric amounts in accordance with their atomic weight rates. The initial components for the insert were thoroughly combined and processed in a garnet slurry that was firmly sealed. Due to the need to fabricate bulk ingots for the $Ge_{35-x}S_{65}Cd_x$ system, the ground combination was put in an electrical roller mill for two hours to obtain very uniform combination blends [15]. The uniform combination was compacted to create highly compressed solid tablets with radii of one and a half cm and a thickness of 3 mm. Each tablet was placed in capsules after being vacuumed at a 10^{-3} bar m and then closed tightly. After that, the capsules were placed in the furnace, and the temperature was raised to 900 degrees Celsius for four hours. The capsules were taken out of the furnace directly into the air, broken, and the molten extracted. Each ingot was then grinded separately, and the samples were pressed under a pressure of six tons per cm square. Then the samples were returned to the oven, heated at a temperature of 200 degrees Celsius for 2 hours, and left inside the oven to cool to room temperature. After that, the samples became ready for tests, where electrical resistivity measurements were made as a function of temperature [16].

3. Results and Discussion

In this work, the temperature dependence on the dc Resistivity and Conductivity of five alloys of $Ge_{35-x}S_{65}Cd_x$ ternary alloy with x = 0, 5, 10, 15, and 20 over a temperature range from 290 to 475 K was studied. The data of the work for the entire range of temperature are well made to fit the model of the thermally activated process. To describe in detail, we used the thermally activated technique over the temperature range of 290K to 475K to determine the conduction mechanism in the samples of the Ge35-xS65Cdx ternary alloy with x = 0, 5, 10, 15, and 20. The diagram of Resistivity vs. 1000/T for the range of T from 290 to 475 K for the five samples is shown in **Figure 1.** The graph is a curve, demonstrating that this system is conducted by a thermally triggered process, and the behavior of the conduction curves indicates that all the alloys under experiment are semiconductors. It is also noted that an increase in the concentration of cadmium in most alloys leads to a decrease in electrical Resistivity in general [17]. As for the ratio x = 15, we notice a significant decrease in the resistivity due to the formation of non-integral bonds, which cause an increase in charge carriers, holes, and electrons. Due to the fact that cadmium is a metallic element, it makes more metallic bonds than necessary. When the ratio x=20 increased, there was parity in the bonds, and thus the compound stabilized. Thus, we conclude that the best replacement ratio is at x=15 because of the bonds formed. We conclude that compound Ge_{20}-S_{65}-Cd_{15} is the best compound in terms of its low resistivity value. [18]

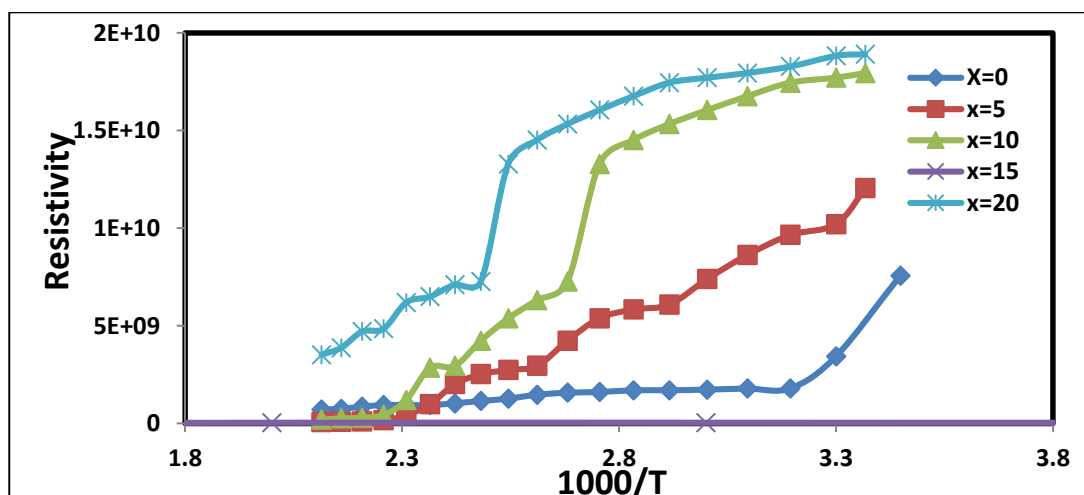**Figure 1**. represents the relationship between the electrical Resistivity as a function of the inverse for the temperatures (1000/T) of the $Ge_{35-x}S_{65}Cd_x$ ternary alloy with x = 0, 5, 10, 15 and 20

The sketch for lin σ_{dc} for 1000/T for the temperature extent from 290K to 475 K is shown in **Figure 2**. This shape indicates that electrons are transmitted in these alloys. via a heated process that is active. It was found that the ratio x=15 is the best ratio because the electrical conductivity has the highest value because of the bonds formed [18].
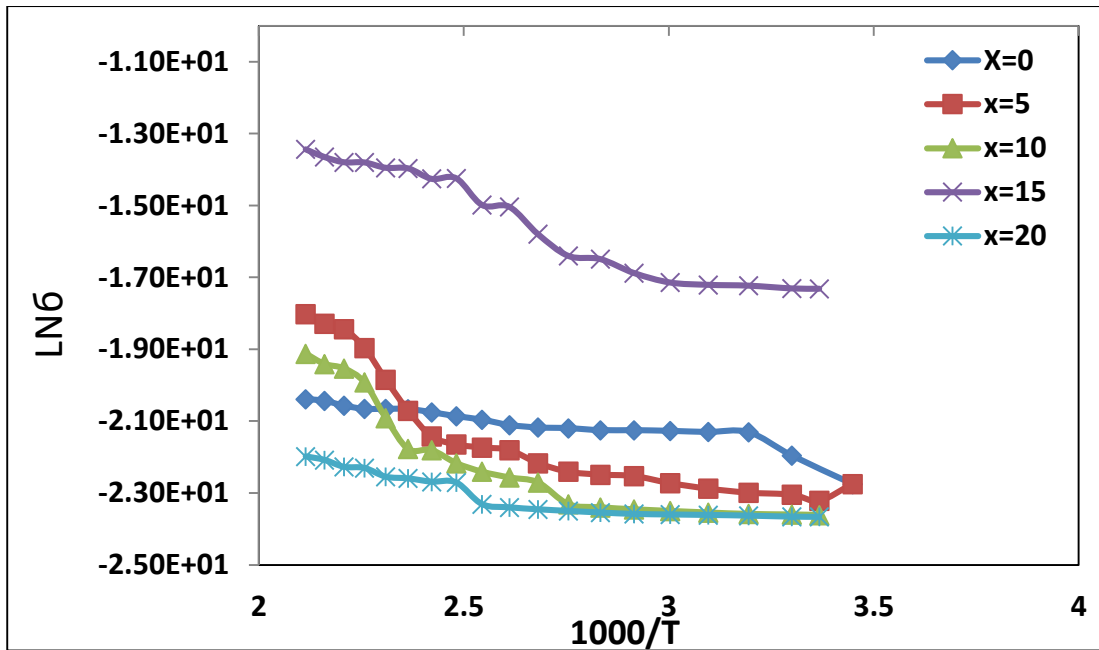
Figure 2. represents the relationship between the Ln continuous conductivity of electricity as a function of the inverse for temperatures (1000/T) of the $Ge_{35-x}S_{65}Cd_x$ ternary alloy with x = 0, 5, 10, 15 and 20

Therefore, the typical relationship that describes conductivity is as follows: [15, 16]. It is noted that the graph consists of curves consisting of three straight lines for all five samples. Fermi at low temperatures (from 290 to 340 K), which requires little energy to activate electrons, and at intermediate temperatures (from 340 to 390 K) that occur between the local planes of the tails of the beams The third conduction mechanism at high temperatures (from 390 to 475 K) occurs among the continuous levels of the conduction and valence bands. The equation that follows [8] describes these three conduction regions.

$$\sigma = \sigma_{01}e^{(-\frac{\Delta E_1}{KT})} + \sigma_{02}e^{(-\frac{\Delta E_2}{KT})} + \sigma_{03}e^{(-\frac{\Delta E_3}{KT})} \qquad (1)$$

where σ_{01}, σ_{02}, σ_{03} represent the Pre- exponential factor calculated from the intercept of Figure 2, and ΔE_1, ΔE_2 and ΔE_3 are the dc calculations of activation energy from the slope of ln σ_{dc} for the (1000/T) sketch for each part.

By using the equation's logarithm (1) on both sides and a graphical representation of (ln σ_{dc}) for (1000/T), we were able to obtain three independent zones with various slopes. matching the 3 parts in Equation (1), if this chart is due to the existing samples of the $Ge_{35-x}S_{65}Cdx$ ternary alloy with x = 0, 5, 10, 15, and 20, one can realize that for each $Ge_{35-x}S_{65}Cdx$ alloy sample The difference between the logarithmic rate of the electrical conductivity (ln σ_{dc}) and the (1000/T) $Ge_{35-x}S_{65}Cdx$ samples yields 3 zones. This, as a result, assumes there are three separate conduct processes. Dominate over certain temperature periods.

A slope for these lines quantifies the activation energy, ΔE, in that region. In addition to extrapolating every streak that locates the(vertical axis) with a mount equal to (lin $\sigma0N$), (where N = 0- 1 and two), and hence, the pre-exponential measurement (σ_{01}, σ_{02}, σ_{03}) is calculable, the first zone, which is the area with the highest temperature, reaches 390 K up to 475K and is also considered the outer semiconductor. The first term of equation (1) provides this temperature range

in this area, the carrier density is equivalent to the self-carrier density. In this case, there are two factors that affect the transition. Measure the retina's vibrations and warmth. The number of carriers rises as the temperature rises. As a result, conduction increases. Contrarily, phonons generated by lattice vibration result in the electronphonon reaction. This reaction is due to the electron being held back, so the electron requires greater energy to operate them, which explains the first region's elevated activation energy amounts [17, 18].

The tow zone starts at temperatures ranging from 340 to 390 K (intermediate temperature zone). The second term of equation (1) describes this area. And is defined as a pure semiconductor, inside the same zone. The carrier density is equivalent to the self-carrier density [18]. The change in mobility is what causes the fluctuation in the d.c. resistance in this zone. The concentration and free path of charge carriers, the low crystallinity, and the small size of the crystals also contribute to this explanation. According to the literature, compositional disorders, distortions, and plane flaws are among the defects that are crucial in lowering conductivity [19, 20].

A third term of equation (1) defines the third zone, which ranges in temperature from 290 K to 340 K. And it represents a low-temperature region. It is defined as the external conductivity of semiconductors, which is caused by the ionization of impurity atoms and extends higher with the depletion of impurities and temperatures. In low- to mid-temperature regions, the thermally assisted mobility of carriers between localized states near the Fermi level is said to be the cause of conduction, according to sources [21]. The energizing forces and pre-exponential factors have been calculated for all samples and for all regions and are listed in **Table 1.**

Table 1. The configuration depend on activity seems and pre- exponential factor σ_0 of 3 governing states Cd consist on $Ge_{35-x}S_{65}Cd_x$ ternary alloy with X = 0.0, 5.0, 10.0, 15.0 and 20.0

X%	E_1(ev)	σ_{01} (Ω.cm)-1	E_2(ev)	(Ω.cm)-1σ_{02}	E_3(ev)	σ_{03} (Ω.cm)-1
0	0.198	$1.8*10^{-7}$	0.094	$1.2*10^{-8}$	0.018	$1*10^{-9}$
5	0.389	$2*10^{-4}$	0.231	$3.2*10^{-7}$	0.096	$3*10^{-9}$
10	0.378	$5*10^{-5}$	0.228	$1*10^{-7}$	0.029	$1.7*10^{-10}$
15	0.330	$4.7*10^{-3}$	0.20	$2*10^{-4}$	0.071	$4*10^{-7}$
20	0.199	$3.9*10^{-8}$	0.067	$5.3*10^{-10}$	0.01	$9.8*10^{-11}$

We calculate using the formula 2. The extended state's density N (E_{ext}) below [18, 19], where the density of the state in the extended area is calculated for all samples using the parameters obtained from **Table 1** after substituting the values of the constants (e is electron charge, m is electron mass, and h is a Black constant) and value σ_{01} for all samples, and the results are tabulated in **Table 2.**

$$N (E_{ext}) = \left[\frac{6m}{e^2\hbar}\right] \sigma_{oext.} \tag{2}$$

$$N (E_{loc}) = \left[\frac{6}{e^2VphR^2}\right] \sigma_{0loc} \tag{3}$$

$$N(E_F) = \left[\frac{6}{e^2 Vph\, R^2}\right]\ \sigma_{o3} \tag{4}$$

As for the local state density at the band's ribbons N (E_{loc}) and near Fermi levels
N (E_F) using equations 3 and 4 [18, 20], they were calculated for all samples using the parameters obtained from Table 1 after substituting the values of the constants (electron charge, the phonon's frequency (Vph) = $10^{13}s^{-1}$.

Between-localize state distance is R hopping ,R = $0.773 \left(\frac{\Delta Ea^{-1}}{N(Eext)(KT)^2}\right)^{\frac{1}{4}}$

and values σ_{01}, σ_{02}, σ_{03} and **Table 2** is a summary of the findings.

For chalcogenide glasses that contain a large percentage of group VI elements, the valence band consists of unshared electron states known as lone pair electrons. [22] Kastner was the first to describe the effects of adding elements to V-VI alloys. He pointed out that the additives affect the width of the tail in the valence band because the valence electrons adjacent to it are more electrically positive. Compared to those, atoms can have greater energy than those located near (adjacent) to electrically charged atoms. In addition, the conduction band's tail changes due to the increase or decrease of the types of bonds present in the alloy [24, 25], and the broadening may not be symmetrical with the valence band and may lead to an increase or decrease in the edge of the conduction band, which affects both the density of localized state N(E_{loc}), extended state N(E_{ext}) at the Fermi level N(E_F), as seen in our results listed in **Table 2**.

Table 2. the Configuration depend on Tail Width ΔE, R, a, N(E_{ext}), N(E_{loc}) and N(E_F) as a result of Cd include of $Ge_{35-x}S_{65}Cd_x$ ternary alloy with x = 0, 5, 10, 15 and 20

X%	Tail Width ΔE(ev)	R(A°) *10^{-5}	a(A°)	N(E_{ext}) 1/ (ev. cm^3)	N(E_{loc}) 1\ (ev. cm^3)	N(E_F) 1/ (ev. cm^3)
0	0.104	0.3	6.061	$5.83*10^{16}$	$9.14*10^6$	$9.22*10^7$
5	0.158	0.06	$5.3*10^{-3}$	$6.48*10^{19}$	$6.5*10^9$	$8.3*10^4$
10	0.150	0.08	$2.1*10^{-2}$	$1.62*10^{19}$	$1.05*10^9$	$3.3*10^5$
15	0.130	0.02	$2.3*10^{-4}$	$1.52*10^{21}$	$2.20*10^{13}$	$3.53*10^3$
20	0.131	0.4	27.97	$1.26*10^{16}$	$1.67*10^5$	$4.26*10^8$

4. Conclusions

The compound $Ge_{35-X}-S_{65}-Cd_X$ was prepared by the molten method. The electrical properties were studied, and it was found that the resistivity in most of the alloys decreases with a decrease in temperature and the conductivity increases with an increase in temperature. This confirms that these alloys are of a semiconductor nature with the presence of mutations in the ratio x=15, because the replacement created additional charge carriers, which led to an increase in conductivity and a decrease in resistivity. It was found that the partial replacement of cadmium had a direct impact on the electrical conductivity variables (σ, activation energy, a, and R). It was also noted that each prepared alloy has three mechanisms: conduction, objective, extended, and Fermi level, and this leads to the existence of three states: local, extended, and Fermi level. And it was found to be affected by the partial substitution of cadmium instead of germanium.

References

1. Wang, Y.; Dai, S.; Mid-infrared supercontinuum generation in chalcogenide glass fibers: a brief review. *PhotoniX*. **2021,** *2, 9,* 34- 45.
2. Noé, P.; Vallée, C., Hippert, F., Fillot, F. & Raty, J.-Y. Phase-change materials for nonvolatile memory devices: From technological challenges to materials science issues. *Semicond. Sci. Technol.* **2018,** 33, 1.
3. Dhanasekaran, V.; Chalcogenides - Preparation and Applications. **2022,** *23*, 45-55
4. Verdy, G. N.; Sousa, V. ; Noé, P.; M. Bernard; F. Fillot; G. Bourgeois; J. Garrione;L. PerniolaImproved electrical performance thanks to Sb and N doping in Se-rich GeSe-based OTS selector devices. *IEEE 9th Int. Mem. Work. , IMW .***2017**,*23*, 45-67
5. Popescu, M. A.; Non Crystalline Chalcogenides.*Springer, Berlin*, **2000,***23*,12- 23
6. Eggleton, B. J. ; Luther, D.; Barry, R.; Kathleen. Chalcogenide photonics. Nature Phot. **2011,** *5*, 141.
7. Tsiulyanu, D.; Ciobanu, M.; Room temperature A.C. operating gas sensors based on quaternary chalcogenides. Sensor. *Actuat. B-Chem*. **2016,***223*, 95–100
8. Lyubin, V.; Klebanov, M.; Feigel, A.; Sfez, B.; Films of chalcogenide glassy semiconductors: New phenomena and new applications. *Thin Solid Films.* **2004,***459*, 183–186
9. Tanaka, K.; Optical nonlinerity in photonic glasses. J. Mater. Sci. Mater. Electron. **2005**, *16*, 633–64
10. Mouawad, O.; Picot-Clémente, J.; Amrani, C.; Strutynski, J.; Fatome, B.; Kibler, F.; Désévédavy, G. Gadret, J.-C. Jules, D. Deng, Y. Ohishi, Smektala F.; Multioctave midinfrared supercontinuum generation in suspended-core chalcogenide fibers. *Opt. Lett.* **2014,** *39*, 2684.
11. Christian R. P.; Uffe, M.; Irnis, K.; Binbin, Z.; Sune, D.; Jacob, R.; Trevor, B.; Slawomir, S.; Nabil, A.; Zhuoqi ,T.; David, F.; Angela, S.; Ole, Bang id-infrared supercontinuum covering the 1.4–13.3 µm molecular fingerprint region using ultra-high NA chalcogenide step-index fibre. *Nat. Phot*. **2014**, *8*, 830–834
12. Nawal, H. k.; Kareem, A. J.; A Study of the Effectiveness of Tin on the Thermal Conductivity Coefficient and Electrical Resistance of Se60Te40-xSnx Chalcogenide Glass. *Ibn Al-Haitham Journal for Pure and Applied Sciences, IHJPAS*. **2023,** *36, 1*, 23-33

13. B. A.; Ahmeda, J. S. Mohammed , R. N.; Fadhila , K. A. Jasima , A. H. Shaban c , A. H. Al Dulaimi, " The dependence of the energy density states on the substitution of chemical elements in the Se6Te4-xSbx thin film, Chalcogenide Letters , **2022,** *19, 4*, 301 – 308,
14. R. K. Nkum , F. K. Ampong and F. Boakye Conduction Mechanism in Amorphous as 2S3",*Journal of Science and Technology*, **2012**, *32, 3*, 11-17
15. Kareem, A. J.; The Effect of Cadmium Substitution on The Superconducting Properties of Tl1-xCdxBa2Ca2Cu3O9-+ δ Compound), *Journal of superconductivity and novel magnetism*, **2013,***26*, 549-552, 9.

16. Aqeel, N. A.; Ahlam, A.; Riyadh, K. C.; Kareem, A. J.; Auday, H. S.; Calculating the Mechanisms of Electrical Conductivity and Energy Density of States for Se85Te10Sn5-xInx Glasses Materials, *Journal of Green Engineering (JGE)*, **2020**, *10, 9*, 5487–5503.

17. Riyadh, K. C.; Sarab, S. J.; Kassim, M. W.; Kareem, A. J.; Auday, H. S.; Fabrication of Ge30Te70-xSbx Glasses Alloys and Studying the Effect of Partial Substitution on D.C Electrical Energy Parameters, *Key Engineering Materials*, **2021**, ISSN: 1662-9795, 9, 163-171.

18. Tariq, J. A.; Kareem, A. J.; The Influence of Annealing Temperature on Density of States, Electrical and Optical Properties of Ge0.2Te0.8Thin Film, *Materials Science and Technology (MS&T),* **2010**, Houston, USA, Texas . October 17-21.

19. Riyadh, K. C.; Sarab, S. J.; Kassim, M. W.; Kareem, A. J.; Auday, H. S.; Fabration of Ge30Te70-xSbx Glasses Alloy and Studying the Partial Substitution on D.C Electrical Energy Parameters, *Key Engineering Materials,* **2021**, *9,9, 3*, 163-171,

20. Stamate, M.; Ph D Thesis, Al.I.Cuza" University, Iasi, Romania, **1999.**

21. Ahmed, B. A.; Mohammed, J. S.; R. N.; Fadhil, K. A.; Jasima, A. H.; Shaban, A. H.; Al Dulaimi, The dependence of the energy density states on the substitution of chemical elements in the Se6Te4-xSbx thin film, Chalcogenide Letters, **2022,** *19, 4,* 301 – 308.

22. A. A. ; Yadav, M.A.; Barote, T.V.; Chavan, E.U.; Masumdar, J.; Influence of indium doping on the properties of spray deposited CdS0.2Se0.8 thin films, *Alloys and Compounds.* **2011**, *509* , 916.

23. Kastner, M.; Bonding, B.; Lone-Pair, B.; Impurity States in Chalcogenide Semiconductors. Phys. *Rev. Lett.* **1972**, *28 (6)*, 355–357.https://doi.org/10. 1103/PhysRevLett.28.355.

24. Nawal, H. K.; , Kareem, A. J.; A Study of the Effectiveness of Tin on the Thermal Conductivity Coefficient and Electrical Resistance of Se60Te40-xSnx Chalcogenide Glass, *Ibn Al-Haitham Journal for Pure and Applied Sciences, IHJPAS.* **2023**, *36*, 1.

25. Baker, E. H.; Webb, L. M.; Preparation and Electrical Conductivity of Some Chalcogenide Glasses at High Temperatures, *J. Materials Science*, **1974,** *9*, 1128-1132

26. Murshed, H.; Fundamentals of Radiation Oncology: *Physical, Biological, and Clinical Aspects. 3rd ed. Academic Press.* **2019**, *23*, 15-21

27. Madlool, S. A.; Abdullah, S. S.; Alabedi, H. H.; Alazawy, N.; Al-Musawi, M. J.; Saad, D.; Optimum Treatment Planning Technique Evaluation for Synchronous Bilateral Breast Cancer with Left Side Supraclavicular Lymph Nodes. *Iranian Journal of Medical Physics.* **2020**, *9*, 45-56.

28. Khan, F. M.; Gibbons, J. P.; Khan's the Physics of Radiation Therapy. 6th ed., *Lippincott Williams & Wilkins;* **2019,** *45*,1–5

29. Faraj, M. K.; Naji N.A.; Alazawy, N. M.; The Efficiency of the Prescribed Dose of the Gamma Knife for the Treatment of Trigeminal Neuralgia. *Interdiscip Neurosurg.* **2018**, *14*, 9–13.

30. Pazdur, R.; Wagman, L. D.; Camphausen, K. A.; Hoskins, W. J.; Cancer Management-A Multidisciplinary Approach. *1st ed. New York: The Oncology Group*; **2003**, *23*, 10-18.